International Journal of Heat and Mass Transfer 58 (2013) 282–291

Contents lists available at SciVerse ScienceDirect

International Journal of Heat and Mass Transfer

journal homepage: www.elsevier.com/locate/ijhmt

Capillary and wetting properties of copper metal foams in the presence of evaporation and sintered walls

Mahmood R.S. Shirazy *, Luc G. Fréchette

Department of Mechanical Engineering, Université de Sherbrooke, 2500 Boul. Université, Sherbrooke, Canada J1K 2R1

ARTICLE INFO

Article history:
Received 21 August 2012
Received in revised form 8 November 2012
Accepted 8 November 2012
Available online 9 December 2012

Keywords:
Heat pipe
Wick
Capillary rise
Evaporation
Internal contact angle

ABSTRACT

An experimental study has been done to define the capillary and wetting characteristics of a novel type of copper metal foam which is to be used as a wick in flat heat pipes for electronic cooling. Unlike other metal foams, a microstructure including micro scale particles and larger capillary paths can be observed in this type of copper metal foam. Due to the significant importance of the capillary properties such as permeability (K) and effective pore radius (r_{eff}) in defining the capillary limit of heat pipes, the rate of rise method based on the measured mass was used to extract these parameters. Foams of different porosities (68–85%) were fully characterized with multiple fluids (water, acetone, and ethanol). The ratio K/r_{eff} was found to be almost 5 times larger than that reported for sintered copper powder, a common wicking material in heat pipes. The impact of evaporation and walls sintered on one side or on both sides of foam strips has been studied in open and partially saturated ambient. The evaporation rate during wicking was measured by subtracting the stored mass of liquid in the foam from the total wicked mass. It was found that the rate of evaporation while the liquid is rising is significantly lower than the evaporation rate of a saturated sample with stationary liquid. It was also observed that sintering copper walls has almost no effect on the capillary rise and on the evaporation rate. By combining measurements done with acetone and water, the internal contact angle of water in hydrogen treated copper foams was found to be lower than on a flat plate and varies from 10° to 37° depending on the foams porosity. This work therefore provides the first characterization of K, r_{eff}, and internal contact angle for these novel metal foams, but also clarifies the conditions under which the rate of rise measurements should be done for proper parameter extraction.

1. Introduction

Wicking materials are the main part of two phase cooling devices increasingly used for thermal management of electronics, such as flat heat pipes and heat spreaders. Due to their capillarity and open pore structure, they carry liquid from the condenser side to the evaporator side in heat pipes or heat spreaders. When one end of a heat pipe is connected to a heat source, such as a hot microprocessor, heat is removed by the evaporation of the liquid enclosed in the pipe. The vapor travels to the other end of the heat pipe where it condenses [1]. The liquid is pumped back to the hot end by the capillary action of the wicking material inserted in the pipe or chamber. The operating range of heat pipes is subjected to several physical limits. For the case of a flat heat pipe utilizing copper metal foam as wicking material, the dominant limit will be capillary limit [2]. This limit is reached when the capillary pumping of the wicking material is not sufficient to supply the required rate of liquid to evaporator and hence, the evaporator will dry out. Therefore, the pumping capacity of the wicking material is a key parameter in the performance of heat pipes. Typical wicking materials include sintered copper powders, copper meshes and more recently copper metal foams. These wicking materials are characterized by their permeability, pore size, porosity, and thermal conductivity. Copper metal foams used in this research (made by Metafoam technologies Inc.) have shown promising results in heat pipes [3] but their wicking performance has not yet been fully characterized.

Capillary properties of a wicking material such as permeability (K) and effective pore radius (r_{eff}) are critical in defining the capillary limit of heat pipes, because their ratio (K/r_{eff}) is a measure of pumping capacity of the wicking material [4]. Permeability can be defined as the porous material resistance against the liquid passing through it. A high permeability will result in a lower liquid pressure drop. Permeability is a pure function of the porous material microstructure and does not depend on the liquid used. Effective pore radius on the other hand, depends on the wetting properties of the liquid in the porous structure. The meniscus profile formed at the liquid–vapor interface of each pore is a function

* Corresponding author. Tel.: +1 819 821 8000x62818; fax: +1 819 821 7163.
E-mail address: reza.shirazy@Usherbrooke.ca (M.R.S. Shirazy).

0017-9310/$ - see front matter © 2012 Elsevier Ltd. All rights reserved.
http://dx.doi.org/10.1016/j.ijheatmasstransfer.2012.11.031

Nomenclature

g	gravity, m/s^2	r_{eff}	effective pore radius, m
h	liquid height, m	t	time, s
K	permeability, m^2	T	foam thickness, m
m	liquid mass, kg	W	foam width, m
$\dot{m}$	liquid mass flow rate, kg/s		
$\dot{m}_e$	evaporation flux from the surface, kg/m^2 s	*Greek symbols*	
m_{evp}	evaporated liquid mass, kg	φ	porosity
m_{st}	stored liquid mass in the foam, kg	μ	viscosity, Pa s
m_{tot}	total wicked liquid mass, kg	ρ	liquid density, kg/m^3
P	periphery, m	Θ	contact angle, deg.
r	pore radius, m		

of the pore structure and also liquid contact angle on the porous material. Therefore, effective pore radius is rather used instead of geometrical pore radius to account for the effect of liquid contact angle. According to the definition of the effective pore radius, it is related to the actual pore radius of a porous material, r, by the liquid contact angle on that material:

$$r_{eff} = \frac{r}{\cos\theta} \tag{1}$$

Effective pore radius is inversely proportional to the liquid contact angle on the solid surface. Hence, a lower liquid contact angle will result in a lower effective pore radius which in turn will increase the K/r_{eff}. Wetting property of a liquid–solid system is defined by measuring the contact angle of the liquid droplet on the solid surface. In the case of water, wettability is expressed by hydrophilic (contact angle less than 90°) and hydrophobic (contact angle more than 90°). It can be concluded that in capillary driven systems such as heat pipes and heat spreaders using water, a hydrophilic wick system is necessary to transport water [5]. It is shown that low wettability of the wicking material directly reduces the critical heat load that can be carried by a heat pipe [6]. Therefore, a good knowledge of these capillary and wetting parameters and a robust method to measure them is important.

The wetting property of a material is commonly determined by measuring the external contact angle of a droplet of liquid on that material (Sessile drop test). This method is not suitable for porous materials since the liquid wicks and disappears under the surface. Furthermore, relating the contact angle on a flat surface to a porous media of the same material can be misleading [7]. The meniscus inside the porous media experiences a complicated 3-D structure which is significantly different from the uniform roughness assumption done in the Sessile drop test. For porous media, a series of methods are available to measure capillary parameters, such as pressure drop measurement for permeability [8,9], or bubble test and rising meniscus for the effective pore radius [4]. One major drawback in these methods is their inability to deliver both K and r_{eff} parameters at the same time and in one test [10].

A potentially more informative method is based on measuring the transient rate of rise of a liquid in a porous medium by measuring its height visually or the increasing mass with a balance [11]. Unlike the rising meniscus which is a static method based on measuring the maximum height of the liquid in a sample, rate of rise method is a dynamic and time dependent method. By fitting a suitable mathematical model to the rate of rise measurements, one can extract both permeability and effective pore radius, or their ratio. This method can also be used to characterize wetting properties of a porous material (internal contact angle) by doing this test with liquids of different surface tension [7,12,13]. The rate of rise method will therefore be used in this work to extract the permeability, effective pore radius and internal contact angle.

When dealing with the transient movement of a liquid in a porous media rising against gravity (vertical sample), a balance between capillary forces wicking the liquid upwards and the opposing inertial, gravity, viscosity and evaporation-induced forces should be considered. Given the complexity of the physics involved, simplified models were initially developed to characterize wicking properties of porous media. By only balancing the viscous pressure drop with the capillary force, and neglecting the other effects, the widely used Lucas–Washburn equation will be obtained [14]. With this method, K and r_{eff} will be obtained as a ratio. To find the values of K and r_{eff} independently, one needs to find the maximum attainable height or mass. This requires fabrication of long samples which may be impractical in many cases. By adding gravitational effects to the Lucas–Washburn equation, Holley and Faghri [10] developed a different equation which permits the extraction of both K and r_{eff} directly (without finding the maximum height or mass). Evaporation taking place on the surface of the porous material will lead to a higher liquid flow rate to accommodate for the evaporated liquid. By assuming a uniform rate of evaporation over the wetted area of their samples, Fries et al. [15] developed a fully implicit solution for all the effects except for inertia, but their experimental results show a 20% difference from their modeling results. Rogacs et al. [16] considered the effects of capillarity, viscosity and evaporation for their thin ($\sim$10 μm) silicon nanowire array and obtained the K/r_{eff} ratio and internal contact angle for this porous structure. Ideally, a suitable model should include the effects of capillarity, viscosity, gravity to extract K, r_{eff}, and internal contact angle, but may also need to account for evaporation in realistic conditions.

Although ignoring the evaporation is useful to simplify the extraction of K and r_{eff}, its omission or the uncertainty on evaporation rate measurements can falsify the results. Understanding the role of evaporation in the rate of rise method is specifically important while dealing with highly volatile liquids like acetone and ethanol. These liquids, due to their low surface tensions, rise easily in copper metal foams in room ambient without the need for any surface treatment. This can alleviate the problem of rapid loss of hydrophilicity in copper-based porous materials when exposed to room ambient. Our tests show that leaving the samples more than 3 min in ambient air has quantifiable effects on the rate of rise of water in these foams. To restore the hydrophilicity, a high temperature hydrogen treatment that may take up to 7 h should be done on the samples, which is not necessary with acetone and ethanol.

Another overlooked aspect is the role of attached walls in the capillary behavior of the porous materials. In practical applications, wicking materials are not used alone and are sintered to a wall to form a two-phase cooling device such as a heat pipe or a heat spreader. A wall can change the flow pattern in the adjacent foams and hence affect the values of permeability. Moreover, the sintered

wall effectively covers the foam surfaces and can alter the evaporation rate from the foam.

Due to the novelty of these copper metal foams, capillary and wicking properties have not been fully understood. This work therefore aims to characterize K, r_{eff}, and internal contact angle of these foams as a measure of their wicking capacity. However, we first need to clarify the role of evaporation and the presence of adjacent walls to ensure the measurement accuracy with the rate of rise method. In this work, copper metal foams with porosities of 68%, 75% and 82%, using DI water, ethanol and acetone as test fluids will be used. To evaluate the effect of adjacent walls, the rate of rise tests have been performed on bare foam strips (no walls) as well as samples with walls sintered on one side or on both sides of the foam strip. To clarify the evaporation effect, high volatility liquids (acetone and ethanol) were used in the open air ambient and in a nearly saturated ambient. Although the rate of evaporation is much lower in a saturated ambient, results will show that the capillary rise behavior is not significantly affected by evaporation, simplifying the extraction of K and r_{eff}. In fact, our results will show that the evaporation rate of a rising liquid in copper metal foams is lower than stationary liquid inside a saturated sample. The method developed herein will be used to fully characterize these novel copper foams including K, r_{eff}, and their internal contact angle with water.

2. Governing equations and models

A complete momentum equation for rise of liquid in a wick should include the capillary pressure, hydrostatic force of the liquid column, viscous friction force in the porous media, inertia of the liquid and the effect of evaporation. Applying force balance on the volume averaged flow, the momentum equation can be written as [15]:

$$\frac{2\sigma}{r_{eff}} = \frac{g}{TW\phi}\cdot m + \frac{\mu}{K\phi(TW\rho)^2}\cdot m\cdot\frac{dm}{dt} + \frac{1}{\rho(\phi TW)^2}\frac{d}{dt}(m\cdot\dot{m}) + \frac{\mu\dot{m}_e(W+T)}{K\rho^3(TW)^3\phi^2}\cdot m^2 \quad (2)$$

The term on the left-hand side is the capillary pressure in which σ is the surface tension (N/m) and r_{eff} is the effective pore radius (m) of the porous material. Capillary pressure is generated by the curvature of the meniscus formed in the pore at the liquid–vapor interface. On the right-hand side, the first term is the hydrostatic pressure of the liquid column in the foam strip in which g is the gravity (m/s^2), T is the foam thickness (m), W is foam width (m), φ is foam porosity, and m is liquid mass in the foam (kg). Friction in the form of a pressure drop is expressed by Darcy's law, as shown by the second term, expressed here in terms of mass. It is a function of viscosity, μ (Pa s), liquid density, ρ (kg/m^3), permeability, K (m^2), and time, t (s). The third term represents the inertial force, expressed in terms of the liquid mass flow rate, $\dot{m}$ (kg/s). It is generally accepted that inertial effects can be ignored compared to other effects [10,15]. Evaporation from the foam surface requires an additional mass flow rate through the foam that should be considered in the governing equation. This extra mass flow rate due to evaporation will induce an additional pressure drop along the foam due to the viscous friction forces. To consider this effect of evaporation, the last term on the right-hand side is added which acts as an extra pressure drop term. The complete derivation of this term was presented by Fries et al. [15], but briefly, it accounts for a non-uniform pressure drop along the foam, assuming a uniform and constant evaporation rate $\dot{m}_e$ over the wetted surface. This evaporation rate per unit area (kg/m^2 s) should be measured separately for each combination of porous material, liquid and surrounding ambient.

Table 1
Mass uptake rate for four limiting cases.

Mathematical models	Solutions
1. Negligible gravitational and evaporation effects (Lucas–Washburn), $B = D = 0$	$m(t) = \sqrt{2At}$
2. Negligible evaporation effects, $B = 0$	$m(t) = \frac{A}{D}\left[1 + W\left(-e^{-1-\frac{D^2t}{A}}\right)\right]$
3. Negligible gravitational effects, $D = 0$	$m(t) = \sqrt{\frac{A}{B}(1 - e^{-2Bt})}$
4.Complete equation (full implicit solution)	$\psi = -4AD - B^2$ $t = \frac{1}{2D}\left[-\ln\left(\frac{-Dm^2-Bm+A}{A}\right)\right]$ $-\frac{B}{2D\sqrt{-\psi}} \times \ln\left[\frac{(-2Dm-B-\sqrt{-\psi})(-B+\sqrt{-\psi})}{(-2Dm-B+\sqrt{-\psi})(-B-\sqrt{-\psi})}\right]$

Ignoring the inertial effects and solving for the rate of change in mass will lead to the following equation:

$$\frac{dm}{dt} = \frac{2\sigma K\phi(TW\rho)^2}{\mu r_{eff}}\cdot\frac{1}{m} - \frac{\dot{m}_e(W+T)}{\rho TW\phi}\cdot m - \frac{KgTW\rho^2}{\mu} \quad (3)$$

which can be expressed in the simplified form:

$$\frac{dm}{dt} = \frac{A}{m} - B\cdot m - D \quad (4)$$

where:

$$A = \frac{2\sigma K\phi(TW\rho)^2}{\mu r_{eff}}, \quad B = \frac{\dot{m}_e(W+T)}{\rho TW\phi}, \quad D = \frac{KgTW\rho^2}{\mu}$$

Fries et al. [15] have presented a fully implicit solution for this equation when it is a function of height $h(t)$. Solution for other limiting cases as a function of $h(t)$ are also available in literature [14,16,17]. By relating mass to the wicking height according to the following equation

$$m = hTW\phi\rho \quad (5)$$

one can readily obtain all the solutions for the mass case (Eq. (4)). Table 1 shows these solutions for the four limiting cases. It can be seen that only models 2 and 4 can directly lead to two parameters K and r_{eff} separately, as opposed to their ratio. If it can be shown that the effect of evaporation is negligible, model 2 may be more appropriate because it is simpler and there is no need to know the rate of evaporation.

3. Materials and methods

The copper metal foams used in this study consist of $16 \times 160 \times 0.7$ mm strips with 68%, 75% and 82% porosity, provided by Metafoam Technologies, Inc. (Fig. 1a). As it can be seen in Fig. 1b and c, the foams have a spherical cluster structure (SCS) with the approximate particle diameter of 10–50 μm, and unlike other types of metal foams, no ligaments can be observed. This morphology is also different than other types of foams which usually have cells shaped as polygons. Instead, the small particles join each other to form clusters that are separated from each other to provide a large-scale porosity in the foam. Within the clusters, we can observe a second smaller scale porosity formed between the particles. The microstructure formed by the small particles and their clusters is therefore characterized by two pore scales and a high surface area.

As a working fluid, water is a logical choice because of its interesting thermal and fluid properties and since it is commonly used in real heat pipes. To better characterize the effect of evaporation and to check the repeatability of the results, acetone and ethanol were also used as test fluids. Copper based porous materials become hydrophobic when exposed to ambient air and a time

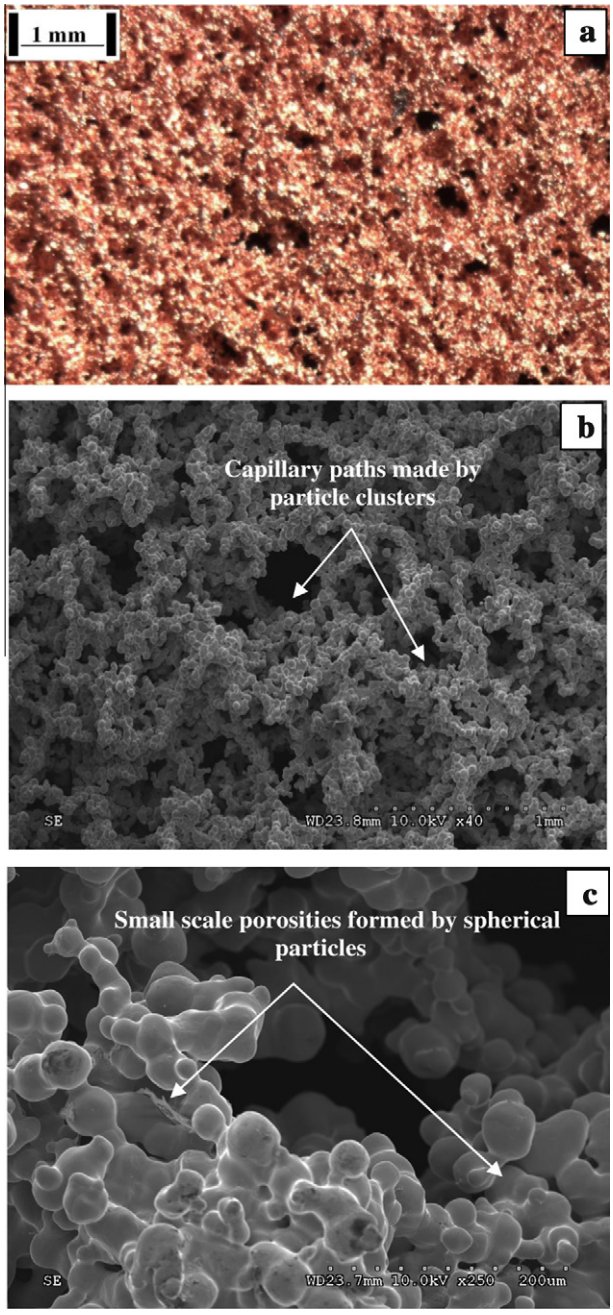

Fig. 1. Morphology of the 75% porosity copper metal foams: (a) A macroscopic view of the copper metal foam (b) capillary paths made by clusters of the spherical particles; (c) small scale porosities formed between the spherical particles.

consuming hydrogen treatment is required to make them hydrophilic again. But unlike water, a low surface energy liquid like acetone (with almost zero contact angle on copper), allows the rate of rise tests to be done without hydrogen treatment because it already imbibes the copper foam samples easily. Moreover, its higher rate of evaporation compared to water makes it easier to characterize the effect of evaporation. Table 2 shows the properties of the liquids used in the experiments.

No cleaning process was performed on the copper foam samples. In order to restore the lost hydrophilicity of copper metal foams, a hydrogen reduction process is however done on the foam samples. A gas mixture of 7% Hydrogen (99.9999% purity) and 93% nitrogen (99.9999% purity) with a total volume flow rate of 150 mL/min is injected into a tube furnace. The heating process

Table 2
Properties of the liquids used in the experiments, 20 °C [18].

	Acetone	Ethanol	Water
Viscosity (Pa s)	0.32e-3	1.17e-3	1e-3
Surface tension (N/m)	0.023	0.022	0.072
Density (kg/m^3)	791.2	788.8	1002

is composed of a ramp from room temperature to 600 °C in 2 h and followed by a 2 h plateau at 600 °C. Then the heat is shut off and the sample is left to cool gradually under the gas mixture. This method was found to be very effective to make the foams hydrophilic and therefore, water was absorbed and could rise in the foams very well.

To evaluate the effect of a wall and evaporation barriers, copper plates (99.9% purity, 0.8 mm thickness) are sintered once on one side and then on the both sides of copper foam samples. Before the sintering process, copper plates are washed with acetone, methanol and IPA to remove all organic contamination. External pressure is applied on the foam and copper plate by a fixture made of two stainless steel plates held by nuts and bolts. Then, the whole package is heated with the same procedure explained above except for the hydrogen concentration which is increased to 20%. This concentration increase is necessary so that hydrogen can better penetrate through the external fixture and reach all the foam pores.

The measurement setups for the rate of rise test based on mass are depicted in Fig. 2. A high precision analytical balance (A&D® model HR-120) with a precision of 0.1 mg is connected to a computer and is used to measure liquid mass uptake in the foam. To measure the stored mass of the liquid (m_{st}) as a function of time (configuration I), the balance is placed on a support so that the foam sample can be mounted vertically from the hook under the balance (Fig. 2a and b). The liquid container placed on the moving stage under the foam sample is raised gradually until the tip of the sample touches the liquid surface. The mass increase is measured in 0.5 s intervals and the measurement is stopped when the measured mass becomes constant (a plateau in the rising liquid graph above ~100 s). In all tests, this plateau is reached when the wetted height is less than the maximum height of the sample (160 mm). The time period between taking out the sample from furnace and starting the test is less than 3 min for all tests with water. For tests with acetone and ethanol, the same procedure but without the hydrogen treatment was employed since their surface energy is low and they easily imbibe the foams.

To evaluate the effect of evaporation of acetone and ethanol, tests were also done under a partially saturated ambient created by a semi-closed transparent container (30 cm height). A small opening (7 mm diameter) was made at the top of the container to attach the samples to the balance. A partially saturated ambient was created by allowing some of the volatile liquid inside the container to evaporate and displace the air, since the vapor density of both acetone and ethanol are greater than that of air. As will be discussed later, this will act as a partially saturated atmosphere and consequently decrease the evaporation rate of acetone and ethanol at the surface of the foam during rate of rise tests. By observing the liquid rise of a test sample, it was found that waiting more than 30 min has no quantifiable effect on the rate of liquid rise and hence, all tests were performed after 30 min of leaving a sample in the container.

In order to measure the total wicked mass of liquid in the foam (m_{tot}), the configuration in Fig. 2c is used (configuration II). Total wicked mass is the sum of the stored mass (m_{st}) and the mass evaporated from the foam surface (m_{evp}). In this configuration, the liquid container is placed directly on the balance and the sample is connected directly to the moving stage. Therefore, the

measured liquid mass at each moment is the sum of stored mass due to capillary and also evaporation from the foam ($m_{tot} = m_{st} + m_{evp}$). To minimize the errors resulting from the evaporation of the liquid in the container, its top is covered and only a slot large enough to insert the sample is left open to ambient. The liquid level inside the container is kept to the maximum so that only the tip of the foam (~2 mm) needs to enter the container. This will ensure that the exposed foam surface is the same as the first configuration (Fig. 2a and b), with minimal impact on the evaporation rate. For configuration II, only ethanol was used as the test liquid because of a stability problem of the balance due to high rate of acetone evaporation. In fact, acetone evaporated so fast from the liquid surface in the container that the balance could not stabilize to provide a starting point. To measure the evaporation rate from saturated suspended foam strips (16 × 50 × 0.7 mm), a number of bare samples and samples with walls sintered to one side (backed) or both sides (double backed) of the strip were tested. They were brought in contact with the liquid, left to become saturated and then detached from the liquid surface. Weight decrease due to evaporation is then recorded in 3 s intervals until the sample is fully dry.

3.1. Corrections on the raw data

3.1.1. Side meniscus effect

As the foam sample touches the liquid surface, a macroscopic meniscus is formed around the end of the sample. This meniscus applies a pulling force to the samples due to the liquid surface tension. The weight measured by the balance is therefore the sum of the actual weight of liquid inside the foam and this pulling force. A simple estimate of this pulling force can be done based on the equation $F = \sigma \cdot P$, where σ is the liquid surface tension and P sample perimeter. For water at 20 °C, a pulling force up to 0.24 g can be expected, which is 20–25% of the whole mass uptake of the foams. Such a significant effect cannot be neglected in the analysis of the results and should be subtracted from the mass uptake. This is done by detaching the sample from the liquid surface after each test (once the sample weight has reached a plateau) and then subtracting the new weight from the weight with the meniscus. This will provide a measurement of the side meniscus force, which is assumed to be constant throughout the whole test. It will be subtracted from all the data points to correct the measured mass. To evaluate the dynamic effect of this meniscus and the possible errors that it may cause, the time required to form this meniscus was measured by a high speed camera. It was ~0.02 s which is much smaller than the first data points in our tests (0.5 s). This effect is present in both test configurations and an example of the effect of this correction on the measured raw data for the total wicked mass measurement (configuration II) can be seen in Fig. 3.

3.1.2. Effect of evaporation from container

For the second experimental setup (configuration II in Fig. 2c), the transient total wicked mass due to both liquid storage and evaporation is measured. Hence, evaporation from the liquid in the container should be subtracted from the results to obtain the values for the foam only. To correct this additional evaporation, the foam sample was detached from the ethanol surface after each test and the mass decrease due to evaporation from the container was recorded. This provides the ethanol evaporation rate from the container. It is assumed constant throughout the test and is therefore subtracted from the balance recorded data (Fig. 3).

4. Results and discussion

4.1. Rate of rise experimental results

Using acetone, ethanol and water as the test liquid and the stored mass measurement experimental setup (configuration I) the rate of rise test has been performed on the foam samples of 68%, 75% and 82% porosity in both open and closed ambient without any sintered wall, a wall sintered to one side (backed) and to both sides (double backed). To account for measurement and foam microstructure variations, tests were done on 2–3 different samples for each porosity and repeated 3 times on each sample. Fig. 4 shows the average of the results for all 3 porosities for acetone as the test liquid. For different foam porosities, the variations seen in rate of rise test results can be attributed to either the sintered wall or the surrounding ambient (open or closed). The capillary effect of the walls can be isolated by analyzing the results in a closed ambient, where evaporation effects are minimized. The results for bare, backed and double backed samples (Fig. 4b and c) in a closed ambient are found to be almost the same for each foam porosity. Although the nominal measurements suggest a slight increase in mass uptake with the number of walls, this is negligible considering the measurement uncertainty. This suggests that the presence of walls adjacent to the foam has no significant effect on the capillary wicking. In the open ambient, the presence of adjacent walls could affect the evaporation rate and therefore the mass uptake. Although the mass uptakes for the open ambient in Fig. 4a (68% porosity) are slightly different, they are practically identical for 75% and 82% porosity foams (Fig. 4b and c). Even for the 68% foam, the effect of this difference in the values of K and r_{eff} will be shown to be negligible considering the measurement uncertainties

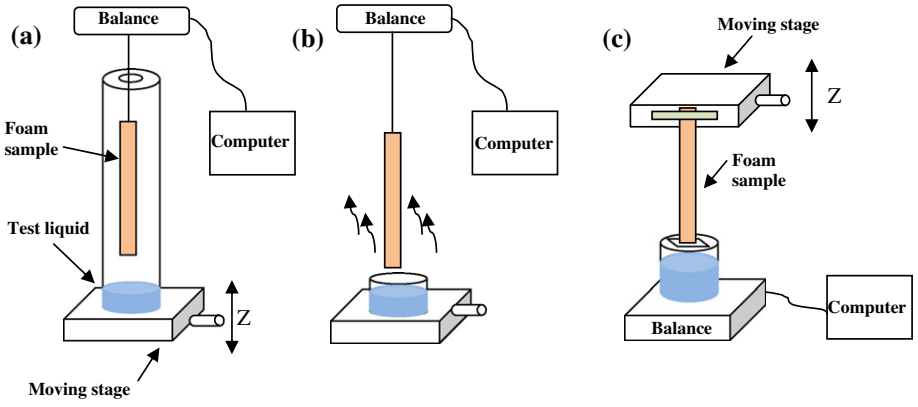

Fig. 2. Different configurations of the experimental setup to measure the rate of rise of a liquid based on mass, done in: (a) semi-closed container for the partially saturated atmosphere; (b) open container for free convection with the ambient; (c) container directly on the balance to measure the sum of capillary forces and evaporated mass from the foam.

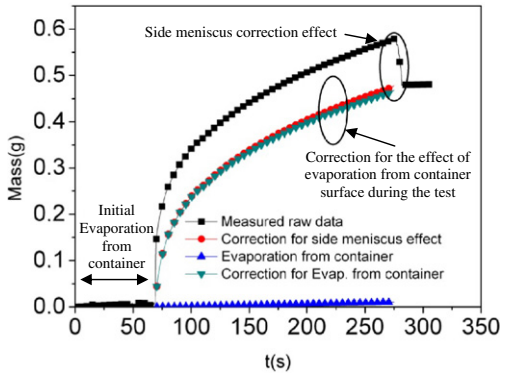

Fig. 3. Measured raw data correction due to side meniscus, evaporation from container during the tests, and initial evaporation from the container before beginning the test.

(Table 4). It can be concluded that enclosing the samples with walls does not change the capillary rate of rise and also is not able to affect the evaporation rate effectively. Considering the almost identical results for different wall configurations (bare, backed and double backed) in each ambient, it can be concluded that doing tests on bare foam samples is adequate to get reliable values for K and r_{eff} by the rate of rise method. However, the mass uptake in the closed ambient seems to be slightly higher than in the open ambient. It can be seen in Fig. 4a and b (68% and 75% porosities) that the highest mass uptake for the closed ambient (partially saturated container). It can be concluded that only by using a partially saturated ambient (closed ambient) can the evaporation rate be sufficiently suppressed to result in a slight change in mass uptake of the foams.

4.2. Evaporation effect

4.2.1. Evaporation rate from stationary liquid

As it was discussed before, evaporation rate of a sample can be measured by measuring the rate of weight loss of a suspended saturated sample. In this case, liquid is stationary in the pores and no fluid dynamics are involved. To investigate the effect of evaporation, acetone and ethanol are used as the test liquids. Fig. 5 shows the non-dimensional measured rate of evaporation of 75% porosity foam samples ($16 \times 50 \times 0.7$ mm) without any sintered copper wall, with one sintered wall (backed) and two sintered walls (double backed) in an open and a closed (partially saturated) environment. It should be noted that for the sake of clarity, Fig. 5 does not show the complete drying curve. The results are non-dimensionalized with respect to the maximum stored mass in the foams at the beginning of each test.

It can be seen in Fig. 5a that the rate of evaporation from the foam is significantly decreased by increasing the saturation level of the surrounding ambient of the sample. It can be observed in Fig. 5b that in the short time interval of the first 200 s, the sample weight in the closed container is almost constant which implies a very low rate of evaporation compared with the sample left in the open environment. Given that the rate of rise test lasts around 100 s, it can be concluded that the closed container has successfully decreased the evaporation rate. On the other hand, the effect of sintered walls on the evaporation rate is very small. Although first one side and then the two sides of the foam sample are covered by the copper plate, only a very slight change in evaporation rate can be observed. To make this effect more clear, Kapton® tape was used to block the uncovered parts of the copper foam (edges and top). Only in this case, the evaporation rate in the open ambient decreases significantly. This shows that in the case of high porosity materials, liquid is trapped in the inner pores during the evaporation and the vapor resulting from the evaporation of the trapped liquid is able to diffuse through the pores and exit the smallest free surface available. In this case, the mass diffusion

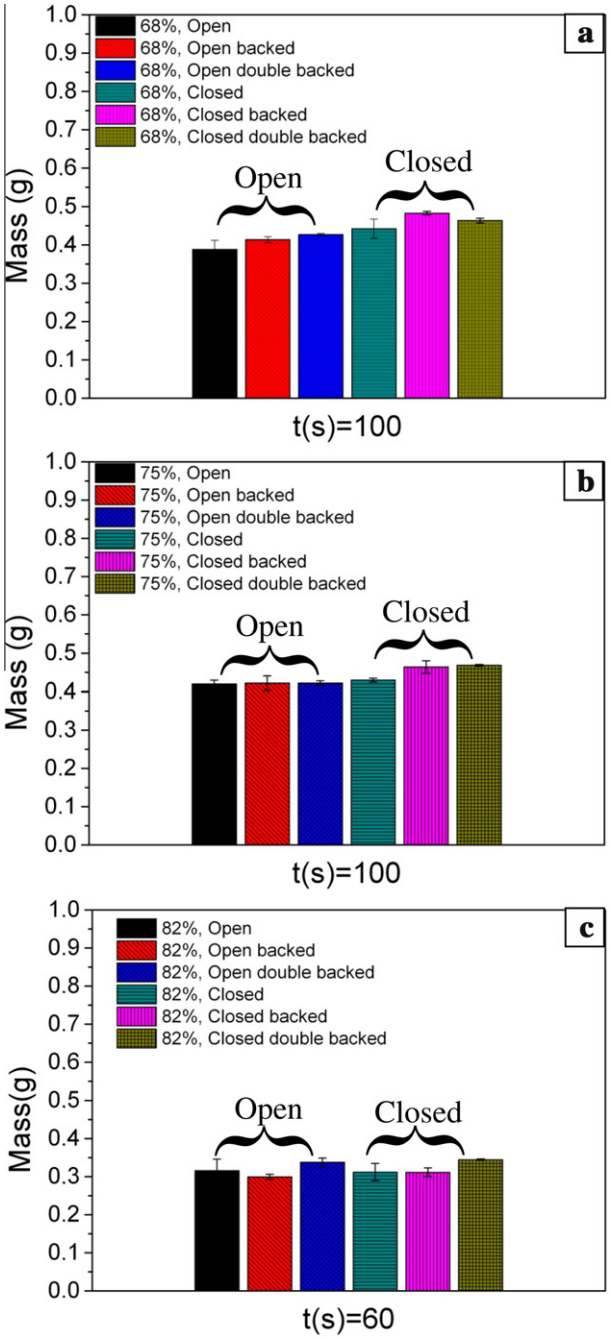

Fig. 4. Rate of rise results for 68%, 75% and 82% porosity foams with acetone in open and closed environments, without any wall, a wall sintered to one side (backed) and to both sides (double backed).

Table 3
Measured evaporation flux for bare samples, $\dot{m}_e$ (kg/m^2 s).

	Open		Closed	
	Acetone	Ethanol	Acetone	Ethanol
68%	3.9e-4	1.1e-4	1.1e-5	2.2e-6
75%	2.9e-4	1.1e-4	1.1e-5	2.9e-6
82%	2.3e-4	1.7e-4	1.2e-5	3.3e-6

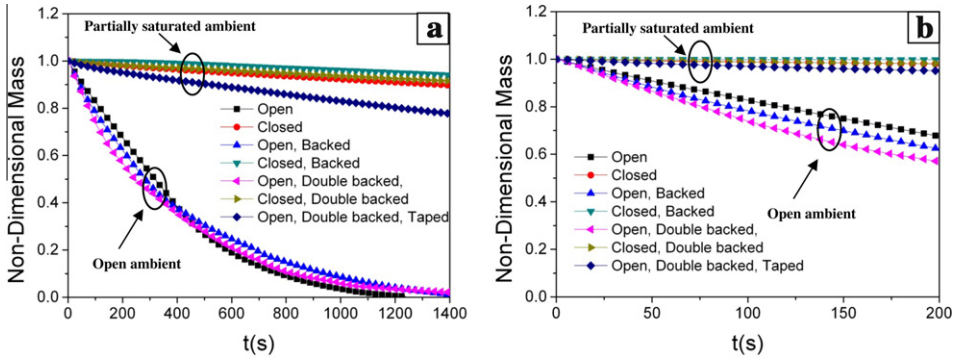

Fig. 5. Non-dimensional evaporated mass measurement of acetone for a 75% porosity foam in open and closed environments with one sintered wall (backed) and two sintered walls (double backed) and covered edges by Kapton® tape, (b) with a close-up on the first 200 s.

Table 4
Permeability K and effective pore radius r_{eff} for foam samples of 68%, 75% and 82% porosities.

		68%				75%				82%			
		K (μm^2)		r_{eff} (μm)		K (μm^2)		r_{eff} (μm)		K (μm^2)		r_{eff} (μm)	
		Mean	STDV	Mean	STDV	Mean	STDV	Mean	STDV	Mean	STDV	Mean	STDV
Acetone	Open	24	2	73.8	0.4	46	7	89.7	0.3	89	11	140.2	0.1
	Closed	21	3	64.6	0.2	45	5	87.7	0.2	96	13	141.1	0.1
	Open, backed	22	2	71.6	0.5	41	5	88.7	0.4	110	10	146.3	0.4
	Closed, backed	20	2	56.0	0.7	42	6	79.6	0.3	127	13	137.5	0.2
	Open, double backed	27	3	73.4	0.2	38	3	87.9	0.6	85	1	128.1	0.7
	Closed, double backed	25	4	66.0	0.4	35	1	78.3	0.9	112	8	106.0	0.2
Ethanol	Open	31	6	89.4	0.9	59	8	104.0	1.0	94	10	135.0	1.0
	Closed	23	6	65.1	0.7	60	9	93.3	0.3	104	9	132.6	0.5
	Open, backed	25	7	66.5	0.9	55	2	84.5	0.9	129	2	135.3	0.2
	Closed, backed	20	3	52.3	0.3	52	1	77.4	1.0	139	11	132.2	0.8
	Open, double backed	40	7	86.4	0.3	60	7	95.5	0.3	105	10	118.8	1.0
	Closed, double backed	32	3	69.1	0.4	45	6	82.1	0.3	104	16	118.9	0.2
Water	Open	19	5	74.8	18.9	51	24	102.0	18.1	74	42	176.0	8.9
Avg.		25	9	–	–	48	13	–	–	105	24		

resistance in the foam is lower than the free convection resistance between the surface and the ambient. Only when the path length required for diffusing the vapor is larger than a characteristic length (the total length of the porous sample in the case of the Kapton® covered sample), then the diffusion rate is affected and hence, the evaporation rate is significantly decreased. Therefore, compared to using a partially saturated ambient, using external walls is not an effective method to decrease evaporation rate. Tests on other foam porosities show the same trend and the results in the form of $\dot{m}_e$ (kg/m^2 s) are presented in Table 3 for the open, and partially saturated ambient.

Although the measured rates of evaporation in Table 3 are significantly higher in the open ambient, the rates of rise of liquids between bare sample in open and closed ambient are the same (Fig. 4). This is surprising because it is expected that the higher rate of evaporation in the open ambient should lead to a lower liquid rise rate compared to liquid rise rate in the closed ambient. This suggests that the evaporation rate from a rising liquid may not be the same as the evaporation rate measured from a stationary saturated sample. If it can be shown that the evaporation rate is lower in the dynamic case (rising liquid), then this will open path to use model 2 (Negligible evaporation) for calculating K and r_{eff}. This will be elaborated in the next section.

4.2.2. Evaporation rate from rising liquid during rate of rise test

In the stored mass setup (configuration I), the balance measures the mass stored in foam at each moment (m_{st}). By employing configuration II, the sum of stored mass in the foam (m_{st}) and evaporated liquid from the foam surface (m_{evp}) is measured. Therefore, the difference between the measurements with configurations I and II provides the evaporation from the foam surface during the liquid rise (Fig. 6). However, a theoretical mass uptake can also be calculated by using the measured evaporation flux of a suspended saturated sample (Table 3) and liquid height. To calculate this mass, the liquid height is visually measured at each moment, multiplied by the evaporation flux in Table 3, and added to the measured stored mass. It is expected that this predicted mass be equal to the measured mass by the total wicked mass setup but it can be seen in Fig. 6 that values of predicted mass are more than the measured ones. This clearly shows that the evaporation fluxes measured for a stationary liquid in a saturated sample (Table 3), will lead to overestimation of the evaporation. In fact, it can be seen that in the short periods of the rate of rise test (~100 s), results of configuration I and II are very close. This suggests that evaporation for this time period can be ignored even for a volatile liquid. Other authors [15] have used the evaporation rate found by measuring the weight loss of a suspended saturated sample in which liquid is stationary. They have found a 20% difference between their measured values and results of the full implicit model with the evaporation term (Eq. (2)). This smaller evaporation rate for a rising liquid compared with stationary liquid can explain this difference.

A possible reason for the lower evaporation rate of the rising liquid compared with stationary liquid can be the difference in the capillary and disjoining pressure in the thin film interface in these two cases. The equilibrium vapor pressure at the liquid–vapor interface of a curved thin film is lower compared with a flat surface at the same saturation temperature due to the disjoining and capillary pressure effect [4]. This will lead to a lower evaporation rate from the vapor–liquid interface. However, Wang et al. [19] show

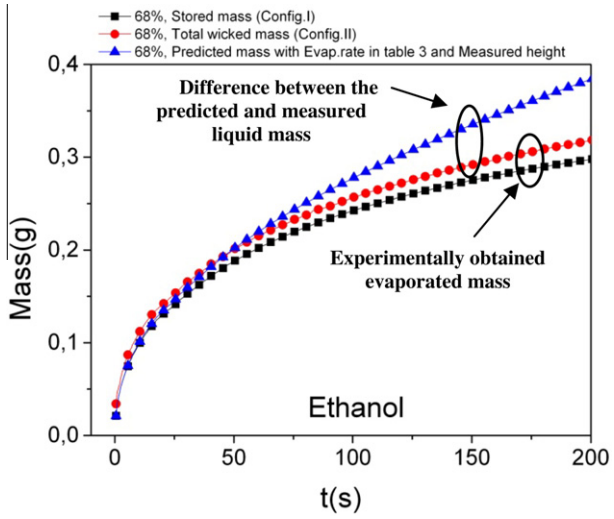

Fig. 6. Rate of rise results for the two setup configurations: stored mass setup (configuration I), total wicked mass setup (configuration II) and predicted mass based on the stationary liquid evaporation rate and measured height for a 68% porosity foam strip.

that for the length scales (or wick dimensions) more than 100 μm this effect is negligible. Given the two pore scales of the foam used in this study, evaporation may occur mainly from the small scale meniscuses formed on the small scale pores (less than 100 μm) in the rising liquid. When the foam is saturated and the liquid is stationary, the bigger pores contribute to the evaporation and the evaporation rate is increased. It should be noted that in a real operating heat pipe, higher evaporation rate and increased temperature may change the meniscus configuration, so this explanation may need to be revisited.

5. Data analysis and parameter extraction

5.1. Permeability and effective pore radius

In order to extract permeability K and effective pore radius r_{eff}, model 2 (negligible evaporation effect) [10] will be used along with measurements from the stored mass setup (configuration I) for the first 100 s of test. Neglecting the evaporation term, Eq. (2) will lead to an ordinary differential equation with two unknowns: permeability and effective pore radius. Solving this simplified equation will lead to the following expression:

$$-\left[\frac{2\sigma}{r}\ln\left(1-\frac{gr}{2\sigma A\phi}m\right)+\frac{g}{A\phi}m\right]=\frac{K\rho^2g^2}{\phi\mu}t \tag{6}$$

It can be seen in Eq. (6) that t can be expressed explicitly as a function of m, liquid properties, sample geometry (assumed constant) and two unknowns: permeability K and effective pore radius r_{eff}. These unknowns can be defined by fitting Eq. (6) to the experimental data. After measuring liquid mass uptake versus time, test liquid properties such as surface tension, viscosity and density and foam sample geometry (width and thickness) are inserted in Eq. (6). The time can then be predicted for a range of K and r_{eff} values. The most representative value of K and r_{eff} is then defined as the pair that minimizes the error, in a least squares sense, between the experimental data (time for a given mass) and predicted time using Eq. (6). The optimization is done over a broad range of K and r_{eff} values to identify the minimum.

Using this approach with acetone, ethanol and water as test liquids, permeability K and effective pore radius r_{eff} are extracted. Results for open and closed ambient and with bare, backed and double backed samples are presented in Table 4. It can be seen that, generally, the results for permeability from acetone, ethanol and water as test liquids are in good agreement. This is expected because permeability is a function of the microstructure of the foams and not the liquid used. The results for effective pore radius between water, ethanol and acetone are different because, as it is shown in Eq. (1), effective pore radius includes the contact angle of the liquid, which is different for different liquids. In fact, unlike permeability, effective pore radius depends on the combination of the liquid and the microstructure. The highest permeability and effective pore radius belong to 82% porosity and the lowest values to 68% porosity foam samples. The impact of the lower evaporation rate in the closed ambient, on the K and r_{eff} can also be seen in this table. Due to the rather small effect of evaporation in the liquid uptake of the foams, the values of K and r_{eff} are generally close in the partially saturated and open ambient. This validates the hypothesis of neglecting the evaporation effect and will confirm the use of model 2 in Table 1.

Table 5 presents the values of K/r_{eff} for different foam samples. As discussed before, unlike permeability (K), effective pore radius depends on the liquid used for the rate of rise test therefore, the values obtained for K/r_{eff} also depend on the liquid. It can be seen that using acetone and ethanol as test fluid, the highest K/r_{eff} ratio belongs to 82% porosity foam which suggests that this foam should have the highest capillary pumping. But in the case of water, 75% foam is more effective for liquid pumping. This can be validated by results presented in Fig. 7 in which mass uptakes of three foam porosities for different test liquids are compared with each other. It can be seen that for acetone and ethanol, the slope of mass uptake of the 82% foam is the highest while for water, the 75% porosity foam can deliver the highest pumping rate (highest slope). It shows that for water as the working fluid, 75% foam is possibly the best foam to attain the highest capillary limit in a heat pipe. For the case of 82% foam, it should be noted that due to its bigger pores the maximum capillary pressure is smaller compared with other foams. However, due to higher permeability (less pressure drop), the initial rate of rise in the first seconds may be quicker than other foam porosities depending on the working liquid. This can be seen clearly in the case of 82% foam with acetone where the slope in the first period of the test (~10 s) is sharper, representing the capillary pumping rate of this porous material with acetone.

Although values of K/r_{eff} depend on parameters such as particle size and porosity, an example in the open literature for sintered copper powder wick with 52% porosity (K/r_{eff} = 0.096 μm with water) [4] can be chosen for comparison. These results show a 5 times increase in K/r_{eff} for 75% porosity foam using water

Table 5
Values of K/r_{eff} (μm) for different conditions and configurations.

	68%			75%			82%		
	Acetone	Ethanol	Water	Acetone	Ethanol	Water	Acetone	Ethanol	Water
Open	0.32	0.35	0.25	0.52	0.56	0.50	0.63	0.70	0.42
Open, backed	0.31	0.37	–	0.46	0.65	–	0.75	0.96	–
Open, double backed	0.37	0.46	–	0.43	0.62	–	0.66	0.89	–

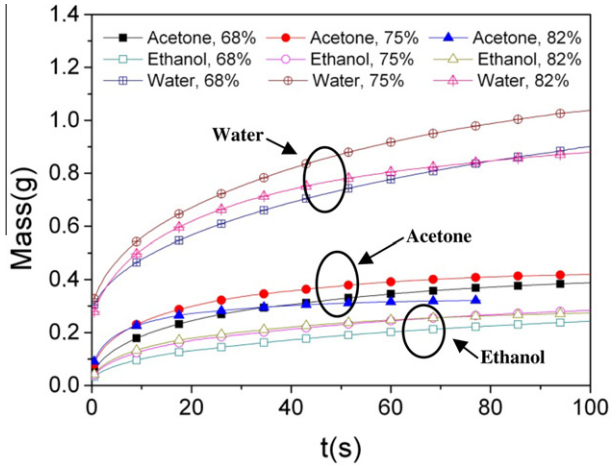

Fig. 7. Mass uptake values for different foam porosities in a closed container with acetone, ethanol and water.

(K/r_{eff} = 0.5 μm) compared to the sintered copper powder wick. While other parameters such as thermal conductivity, wick thickness and wall contact quality are also important, this clearly shows the potential enhancement in the capillary pumping that can be obtained by using these foams.

5.2. Internal contact angle

Water is the typical working liquid for heat pipes and knowing its internal contact angle can provide insight on the wicking behaviour. Contact angle measurements show a value of 47° for water on a hydrogen treated (hydrophilic) copper plate sample, but these may be different in porous structures. Reducing this value could potentially increase the heat pipe performance by increasing K/r_{eff}. The approach to extract the internal contact angle is to use a low surface energy liquid (near zero contact angle) to measure the effective pore radius and then calculating r in Eq. (1). The use of ethanol for this comparison was ruled out because the contact angle of 95% ethanol (employed in this study) is higher than zero. Collier and Thome [20] present the values of contact angle of 14–19° for ethanol on a copper surface. Moreover, Fan et al. [21] measure a contact angle of 10–15° for 85% ethanol in atmospheric conditions on a copper surface. Our tests in the laboratory show the same non-zero contact angle for ethanol on a copper plate. Therefore, the 'near zero' contact angle assumption would be violated. However, our measurements show that acetone has a zero contact angle on a flat copper surface, making it a good reference fluid to extract r. The cosine of the internal contact angle for water is therefore simply the ratio of the effective pore radius of acetone and water. It can be seen in Table 6 that these values are smaller than the water contact angle on a flat copper surface. This is due to the morphology of the pores and the interactions of the liquid with the microstructure. Moreover, as the porosity increases, internal contact angle increases also. This can be attributed to the close to zero contact angle of the liquid in small pores [22]. As the porosity increases, the pores become larger and the effect of the microstructure becomes less dominant. It can be seen that although the hydrogen treatment is obviously able to render the surfaces hydrophilic, this hydrophilicity is not perfect (zero contact angle). Developing more effective methods for making the copper hydrophilic can increase the capillary pumping, especially for higher porosity foams (in this case 82% foam). A combination of high porosity and low liquid contact angle could increase the operating limit of the heat pipes by providing bigger paths for vapor to escape, less pressure drop and better capillary pumping.

Table 6
Internal contact angle of water in an open ambient.

Porosity	$r_{eff,\ acetone}$ (μm)	$r_{eff,\ water}$ (μm)	$\theta_{water,int}$
68%	73.8	74.8	~9
75%	89.7	102	~28
82%	140.2	176	~37
Copper flat surface	–	–	~47

6. Conclusion

Permeability, effective pore radius and internal contact angle of copper metal foams are obtained by measuring the rate of mass uptake with acetone, ethanol, and water as test liquids. Specific attention was given to the role of evaporation and the presence of walls to evaluate their importance on the vertical rising of a liquid in a porous material. The following conclusions can be drawn from this study:

(1) Permeability and effective pore radius are obtained by doing the measurements in the open ambient and using model 2 in Table 1 (negligible evaporation) for the foam porosities of 68%, 75% and 82%. The highest permeability and effective pore radius were found for the 82% porosity and the lowest values for 68% porosity foam samples. Using acetone and ethanol as test fluids, the highest K/r_{eff} ratio belongs to 82% porosity foam which suggests that this foam should have the highest capillary pumping. But in the case of water, 75% porosity foam is more effective for liquid pumping. Its K/r_{eff} ratio is almost 5 times bigger than sintered copper powder, which makes it a very promising wicking material.
(2) The rate of evaporation of acetone and ethanol from the rising liquid is significantly lower than that measured for stationary liquid in a saturated foam sample. For a rising liquid, this may be due to lower evaporation rate from the meniscuses formed on the smaller scale pores (less than 100 μm) caused by higher disjoining and capillary pressures. This allows evaporation effects to be neglected in the rate of rise test even for highly volatile liquids like acetone. This way, permeability and effective pore radius can be extracted directly by using model 2 in Table 1, which ignores the evaporation effect.
(3) Sintering copper walls to the copper metal foams has almost no effect on the capillary rise behavior and the evaporation rate. Hence, covering most of the foam surfaces does not hinder the evaporation rate. Only by putting the samples in a semi saturated ambient can a significant change in evaporation rate be observed. This suggests that the foams are very efficient mass transport media with low internal mass diffusion resistance.
(4) The non-zero internal contact angle of water in the copper porous foams is seen to be smaller than the water contact angle on a flat piece of copper. It is caused by the morphology of the foams and the interactions of the liquid and microstructure. Decreasing the internal contact angle can change the ratio of K/r_{eff} which would favor more porous foams.

This work has therefore not only provided capillary properties of copper metal foams for the first time, but also clarified the conditions under which the rate of rise method should be conducted to properly extract these properties. Although the effects of evaporation and the presence of an adjacent wall were found to have a negligible impact on the rate of rise measurement, these effects may be different at high heat rates typically seen in heat pipes.

In particular, evaporation during the operation of a heat pipe may be a function of its pumping rate, since this work has shown the evaporation rate to be different for wicking versus saturated foams.

Acknowledgments

This research was jointly funded by NSERC and Metafoam Technologies Inc. We are grateful for the support and guidance of Dominic Pilon. The contributions of Stéphane Gutierrez for SEM imaging and Louis-Simon Malo for testing are also greatly appreciated.

References

[1] G.P. Peterson, An Introduction to Heat Pipes: Modeling, Testing, and Applications, Wiley-Interscience, 1994. p. 368.
[2] M.R.S. Shirazy, L.G. Fréchette, A parametric investigation of operating limits in heat pipes using novel metal foams as wicks, ASME 2010 3rd Joint US-European Fluids Engineering Summer Meeting and 8th International Conference on Nanochannels, Microchannels, and Minichannels FEDSM2010-ICNMM2010, (2010).
[3] D. Pilon, High Heat Load Capacity Copper Foam Wick Structures, AMD Technical Forum and Exposition, Taipei, 2009.
[4] A. Faghri, Heat Pipe Science and Technology, first ed., Taylor & Francis Group, Great Britain, 1995. p. 854.
[5] P.d. Gennes, F. Brochard-Wyard, D. Quere, Capillarity and Wetting Phenomena: Drops, Bubbles, Pearls, Waves, Springer, 2004.
[6] S. Wong, Y. Lin, Effect of copper surface wettability on the evaporation performance: tests in a flat-plate heat pipe with visualization, Int. J. Heat Mass Transfer 54 (2011) 3921–3926.
[7] V. Gurau, M.J. Bluemle, E.S. De Castro, Y. Tsou, J.A. Mann Jr., T.A. Zawodzinski Jr., Characterization of transport properties in gas diffusion layers for proton exchange membrane fuel cells. 1. Wettability (internal contact angle to water and surface energy of GDL fibers), J. Power Sources 160 (2006) 1156–1162.
[8] D. Pilon, S. Labbe, J. Touzin, B. Marsan, R. Panneton, L. Frechette, E. Gros, Characterization of high surface area open-cell metal foams and application to thermal management and electrochemistry, in: 5th International Conference on Porous Metals and Metallic Foams, MetFoam 2007 (2007) p. 501.
[9] L.F. Berti, P.H.D. Santos, E. Bazzo, R. Janssen, D. Hotza, C.R. Rambo, Evaluation of permeability of ceramic wick structures for two phase heat transfer devices, Appl. Therm. Eng. 31 (2011) 1076–1081.
[10] B. Holley, A. Faghri, Permeability and effective pore radius measurements for heat pipe and fuel cell applications, Appl. Therm. Eng. 26 (2006) 448–462.
[11] L. Labajos-Broncano, M. Gonzalez-Martin, J.M. Bruque, C. Gonzalez-Garcia, Comparison of the use of Washburn's equation in the distance-time and weight-time imbibition techniques, J. Colloid Interface Sci. 233 (2001) 356–360.
[12] B.R. Friess, M. Hoorfar, Measurement of internal wettability of gas diffusion porous media of proton exchange membrane fuel cells, J. Power Sources 195 (2010) 4736–4742.
[13] V. Gurau, J.A. Mann, Technique for characterization of the wettability properties of gas diffusion media for proton exchange membrane fuel cells, J. Colloid Interface Sci. 350 (2010) 577–580.
[14] J. Schoelkopf, P.A.C. Gane, C.J. Ridgway, G.P. Matthews, Practical observation of deviation from Lucas–Washburn scaling in porous media, Colloid Surface A 206 (2002) 445–454.
[15] N. Fries, K. Odic, M. Conrath, M. Dreyer, The effect of evaporation on the wicking of liquids into a metallic weave, J. Colloid Interface Sci. 321 (2008) 118–129.
[16] A. Rogacs, J.E. Steinbrenner, J.A. Rowlette, J.M. Weisse, X.L. Zheng, K.E. Goodson, Characterization of the wettability of thin nanostructured films in the presence of evaporation, J. Colloid Interface Sci. 349 (2010) 354–360.
[17] N. Fries, M. Dreyer, An analytic solution of capillary rise restrained by gravity, J. Colloid Interface Sci. 320 (2008) 259–263.
[18] A.W. Adamson, A.P. Gast, Physical Chemistry of Surfaces, sixth ed., United States of America, 1997. p. 808.
[19] H. Wang, S.V. Garimella, J.Y. Murthy, Characteristics of an evaporating thin film in a microchannel, Int. J. Heat Mass Transfer 50 (2007) 3933–3942.
[20] J.G. Collier, J.R. Thome, Convective Boiling and Condensation, third ed., Oxford University Press, 2001.
[21] L. Fan, X. Yuan, C. Zhou, A. Zeng, K. Yu, M. Kalbassi, K. Porter, Contact angle of ethanol and *n*-propanol aqueous solutions on metal surfaces, Chem. Eng. Technol. 34 (2011) 1535–1542.
[22] C. Byon, S.J. Kim, Capillary performance of bi-porous sintered metal wicks, Int. J. Heat Mass Transfer 55 (2012) 4096–4103.